Electronics Letters

LETTER OPEN ACCESS

Nanosecond Pulsed, Large-Array, Light Emitting Diode Light Source

Jendrik Schmidt[1] | Georg Ludwig[1] | Jan Menke[1] | Enno Peters[1] | Maurice Stephan[1] | Oliver Zielinski[2]

[1]Institute for the Protection of Maritime Infrastructures, German Aerospace Center (DLR), Bremerhaven, Germany | [2]Helmholtz-Zentrum Hereon, Geesthacht, Germany

Correspondence: Jendrik Schmidt (jendrik.schmidt@dlr.de)

Received: 7 November 2025 | **Revised:** 13 April 2026 | **Accepted:** 20 April 2026

ABSTRACT

Nanosecond LED light sources require active carrier sweep-out drivers in order to reduce the optical fall time down to a few nanoseconds. For applications in direct time-of-flight systems, it is aimed for a high power LED spotlight capable of emitting 4–8 ns pulses. Therefore, six selected LED driver circuits with 3 A peak current are compared and discussed in terms of pulse shape, efficiency and scalability for a large array spotlight. Inductive sweep-out drivers and totem-pole drivers for single LEDs achieved optical fall times between 2.5 and 5.3 ns at 6 ns pulse width (fwhm). A timing and power analysis on a spotlight consisting of 89 LEDs demonstrates the feasibility of the totem-pole driver in a 62 mW array at 6 ns pulse width and a pulse frequency of 1 MHz.

1 | Introduction

Nanosecond light pulses are required in many applications, for instance optical communication [1, 2], fluorescence lifetime microscopy [3], LiDAR [4, 5] and photoacoustic signal acquisition systems [6, 7]. As optical rise and fall times, as well as pulse energy are critical performance parameters, laser diodes are typically used.

Typically, in order to achieve nanosecond LED pulses, two driver design measures are applied. (1) An intended current overshoot, referred to as current peaking, improves the optical rising time at LED turn-on. (2) At LED turn-off, a reverse current sweeps out the remaining minority charge carriers. Since the remaining charge is a function of LED current, an effective sweep-out becomes increasingly important when pulsing high power LEDs. A well-known method is to actively short-circuit the LED at turn-off, for example, by adding a PMOS FET between the LED terminals. The FET provides a low resistance path for charge equalization, with the potential of improving fall times by approximately 80%, for instance from 56 to 10 ns [8]. Other authors proposed to force a sweep-out current by actively toggling FETs [3], adding an inductance parallel to the LED [9] or utilizing the nearly ideal diode behavior of Schottky diodes [10, 11]. All of the above mentioned sweep-out circuits were applied to low-side LED drivers. However, Veledar et al. [12] achieved optical fall times between 1.87 and 3.80 ns in a high-side driver configuration (Darlington circuit) with different pulse shaping techniques based on diodes and inductance.

These drivers were designed and evaluated in single LED setups. However, high optical power applications, for instance underwater range-gated (flash LiDAR), which was addressed in this study, require a spotlight consisting of multiple LEDs. Previous estimations concluded, that for a sufficiently high pulse energy, a large array of approx. 100 synchronized LEDs is required [13]. This results in additional design hurdles, like board area required per driver, which is typically less of an issue in high-speed single LED drivers.

Therefore, this study aims to develop a nanosecond LED driver circuit, that achieves 4–8 ns optical pulses at peak currents around

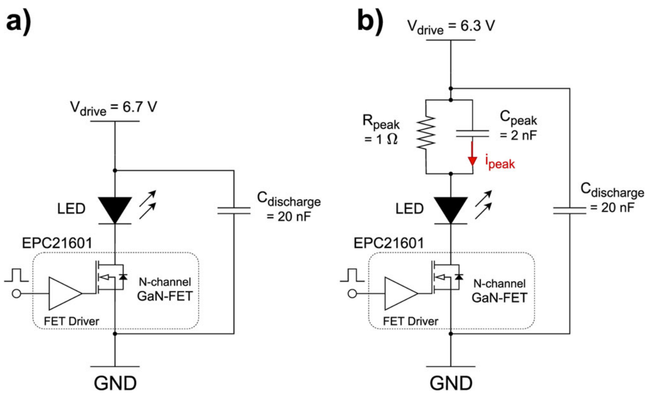

FIGURE 1 | Tested simple low-side LC-resonant drivers (a) without and (b) with R || C peaking circuit.

3 A at up to 1 MHz pulse frequency. Six selected single LED driver designs are experimentally evaluated and their advantages and drawbacks are compared with respect to their use in a large LED array configuration. Also, the performance of a large array spotlight is experimentally evaluated and compared to a single driver.

2 | Evaluated LED drivers

2.1 | LC Resonant Drivers (Used as Reference)

A simple way to achieve short optical pulses is by discharging a capacitor through a low-side FET. The capacitance in series with the parasitic inductance in the power loop forms an LC oscillator. Pulse current and width are controlled via $C_{discharge}$ and V_{drive} selection (Figure 1a). All low-side drivers considered in this study are switched with the EPC21601 integrated GaN-FET and driver, providing sub-nanosecond rising and falling edges in a small 1.5 x 1.0 mm^2 package. For a better current control and enhancement of the rising edge, current peaking is typically implemented, allowing a surge current i_{peak} at FET turn-on to bypath the current limiting resistor R_{peak} through a parallel capacitor C_{peak} (Figure 1b). These drivers require a very low amount of components and board space, making them ideal for large arrays. However, the simple LC resonant drivers do not provide any sweep-out measures. Therefore, they are regarded as reference in this study, allowing to evaluate the intrinsic LED turn-off time and the pulse shape improvements by the other drivers.

2.2 | Inductive Sweep-Out Drivers

Adding an inductance and a resistor in parallel to the LED has been shown to effectively reduce the turn-off time of a near-infrared LED down to 2.5 ns at a pulse current of 2 A [9]. At FET turn-off, the decaying magnetic field of the parallel inductance induces a reverse current, actively sweeping out the remaining LED minority charge carriers. This driver design was adopted for the study presented here and evaluated with and without an added current peaking circuit (Figures 2a and 2b). This sweep-out solution is attractive for large arrays, because it is based on only two additional passive components.

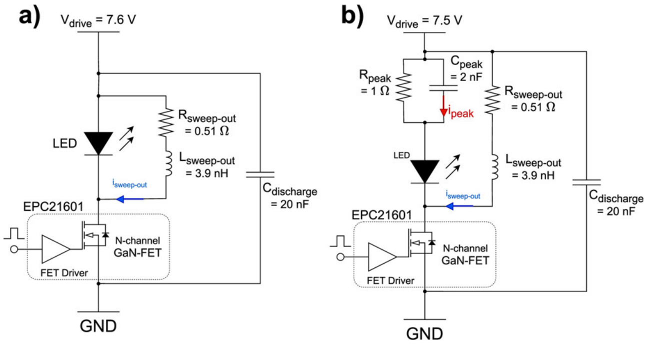

FIGURE 2 | Tested RL-parallel, inductive sweep-out drivers (a) without and (b) with R || C peaking circuit.

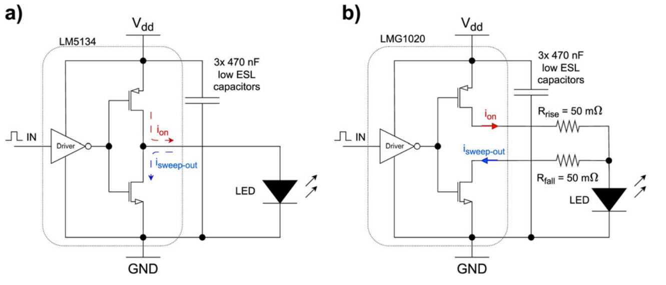

FIGURE 3 | Tested totem-pole driver configurations using the (a) LM5134 gate driver and (b) LMG1020 gate driver IC.

2.3 | Totem-Pole Drivers

Another technique to reduce the LED optical fall time is to actively short circuit the LED after turn-off. In contrast to previous work [8], we propose to drive the LED with the LM5134 and LMG1020 totem-pole gate drivers by Texas Instruments (Figures 3a and 3b). In this case, the LED is high-side driven when turned-on and when the driver is turned off, its anode is shorted to the cathode and thus to ground. Both gate driver integrated circuits (ICs) provide the required compactness and already handle dead time, preventing a short circuit of the driver supply. Through the external resistors R_{rise} and R_{fall} at the separate high-side and low-side pins of the LMG1020, the current rise and fall time are controlled.

3 | PCB Layout Considerations

When designing the LED drivers, a careful PCB layout is required in order to keep the influence of parasitics on driver performance as small as possible. In particular, the parasitic inductance of the LED power and sweep-out current loops impact rise and fall times. Therefore, the loop areas of the wide trace current paths (especially the sweep-out loop) were minimized while preventing current crossings and utilizing return paths via 2nd layer ground planes.

4 | LED Selection and Measurement Setup

For the addressed underwater lighting application, the AMS Osram KB CSLNM1.14 (blue), KT CSLNM1.13 (green) and KR

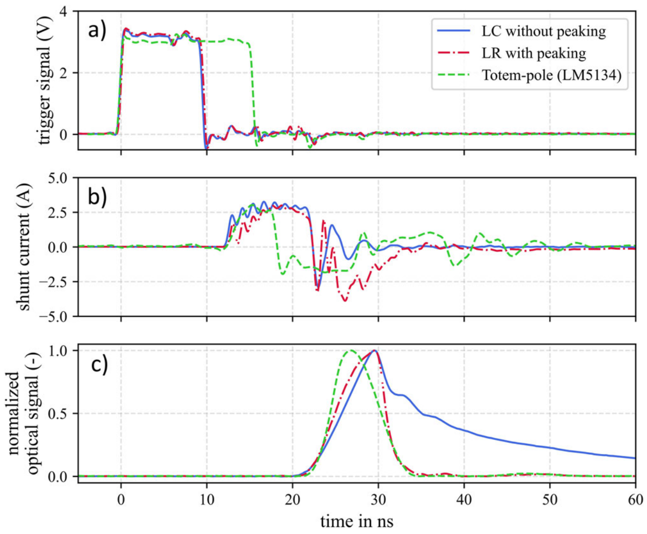

FIGURE 4 | Time waveform analysis for LC, LR and totem-pole drivers, aiming for 6 ns fwhm optical pulses at 3 A peak current and 100 kHz repetition rate: (a) 3.3 V trigger signal, (b) shunt (LED) current and (c) resulting optical pulses.

CSLNM1.23 (red) LEDs were used, as they sustain high current densities (surge current ratings of 4.5, 4.0 and 3.3 A) in a small 9 mm^2 ceramic package. A small carrier lifetime, LED junction capacity and effective series inductance are preferred. However, they are often not provided in datasheets. The following comparison is presented exemplary for the red LED, as all three variants show comparable pulse shape results.

The above introduced LED drivers were realized with component values as indicated in Figures 1–3 and characterized at a pulse frequency of 100 kHz. A subsequent frequency analysis showed that there is no relevant pulse shape and pulse energy variation between 1 kHz and 1 MHz. The drive voltage was adjusted for an LED pulse current of 3 A, which was measured over a shunt resistor with a 1.5 GHz differential probe and an oscilloscope at 12.5 Gsample/s. The optical pulse shape was measured with a fiber-coupled UPD-200-SP photodiode with a bandwidth higher than 2 GHz. The LED driver was directly triggered from a modified Jim Williams short pulse generator [14]. Trigger pulse width was adjusted such, that the fwhm optical pulse length t_{fwhm} corresponds to 4, 6, 8 ns. To calculate the driver efficiency, the photodiode was replaced with a Thorlabs SB120C sensor head connected to a Thorlabs PM100 USB power meter, measuring the average optical output, which was divided by the average electrical input. The resulting efficiencies exclude the trigger circuit.

5 | Experimental Results

5.1 | Electrical and Optical Pulse Shapes

The three driver types introduced above showed characteristic electrical and optical waveforms. Generally, pulse shape variations due to added peaking circuits within these categories are minor. Figure 4a–c shows a consolidated waveform analysis of the (a) input trigger signals, (b) LED currents and (c) emitted optical pulses of the three tested driver topologies. The current for the LR driver with peaking is measured over R_{peak}, not including the peaking current over C_{peak}. Also, the propagation delay of the photodiode receiver is not calibrated and therefore, delay between electrical and optical pulses is not exactly measured. After ≈ 12 ns propagation delay, all current pulses approach a 3 A plateau followed by a sharp cut-off. At turn-off, each driver topology leads to different current profiles and therefore different optical pulse shapes.

TABLE 1 | Rise and fall times of tested LED drivers at 6 ns optical pulse width, 3 A LED peak current and $f_{pulse} = 100$ kHz.

Driver	t_{rise} (ns)	t_{fall} (ns)
LC low-side[a]	6.7	40.8
LC with peaking[a]	6.6	42.2
LR parallel	6.2	3.5
LR parallel with peaking	5.3	2.5
Totem-pole LM5134	3.8	4.6
Totem-pole LMG1020	4.6	5.3

[a]A pulse width of 6 ns could not be achieved because of too slow fall time.

At turn-off, the simple LC driver goes into a high impedance state, quickly cutting the LED current off without a longer reverse sweep-out phase. This causes minority charge carriers to stay and recombine within the LED, leading to a long optical fall time t_{fall} around 40 ns (Figure 4c), preventing emission of measurable optical pulses shorter than ≈ 10 ns.

In contrary, the current of the LR driver has an approximately 10 ns long sweep-out (reverse) current phase after turn-off, leading to $t_{fall} = 2.5$ ns for a 6 ns optical pulse (red lines in Figures 4b and 4c). Additionally, the circuit requires careful design, since it is prone to current oscillations, because of the parallel inductance in forming an LC oscillator with the LED junction capacity.

The totem-pole driver provides a significantly shorter current pulse than the LR driver, for an equivalent 6 ns fwhm optical pulse, which can be explained by the longer fall time, widening the optical pulse width. Like the LR driver, the current curve shows an approximately 10 ns long sweep-out (reverse) current phase after turn-off, leading to an optical fall time of 4.6 ns. The longer fall time compared to the LR driver is a consequence of shortening the LED, but not actively forcing a higher reverse current. Furthermore, a second, approximately 10 ns long positive current pulse can be seen for the totem-pole driver (green line in Figure 4b). Since no second optical pulse is emitted, this could be explained by the reverse recovery current of the ESD diode inside the LED. The achieved rise and fall times of tested drivers are summarized in Table 1.

5.2 | Pulse Shape Variation With Pulse Width

Operating the LED drivers at optical pulse widths of 4 and 8 ns yielded comparable results to 6 ns fwhm, with an overall trend towards shorter rise and fall times at $t_{pulse} = 4$ ns and slower

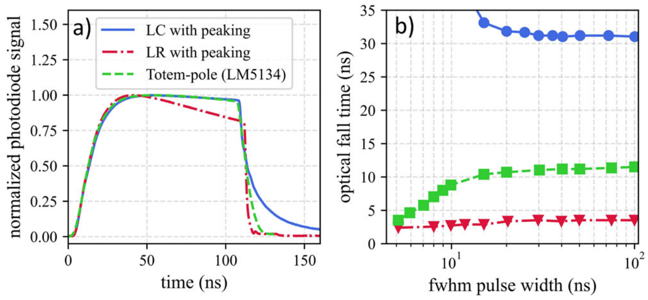

FIGURE 5 | Pulse width variation analysis: (a) optical pulse shapes measured at 100 ns fwhm pulse width; (b) fall times at different optical pulse widths.

edges at t_{pulse} = 8 ns. At drastically increased pulse widths, the pulse shapes can change significantly. Figure 5a shows 100 ns fwhm optical pulses of all three driver topologies ($C_{discharge}$ had to be increased to 3x 470 nF for the LC and LR drivers to provide enough pulse energy). In contrary to the short pulses, the 100 ns pulses reach an almost steady-state optical plateau. The stronger declining LR sweep-out driver plateau (red line) results from the parallel, low impedance LR path limiting driver efficiency at longer pulses.

All drivers result in $t_{rise} \approx$ 20 ns for pulse widths larger than 30 ns. At shorter pulses (e.g., in Figure 4c), the rise time is shorter, because the current is turned off before the optical peak power is reached. The fall time of the simple LC driver levels off around 31 ns. Towards shorter pulses it even increases, as the exponential decay is less steep. Both, the LR and totem-pole drivers are capable of maintaining a reduced fall time at longer pulse width (see Figure 5b). Up to approximately 20–30 ns wide pulses, their fall times increase until they stabilize at $t_{fall} \approx$ 11 ns (LM5134 totem-pole driver) and 3.6 ns (LR driver with peaking). The early increase of fall times can be explained by an increasing number of injected carriers which have to be swept out.

5.3 | Pulse Energy and Efficiency

Because of the high number of drivers per area, the driver efficiency becomes increasingly important in large arrays. In general, a trend of optical pulse energy and driver efficiency increasing with pulse length was obtained for all drivers in the 4–8 ns range. Table 2 summarizes the obtained pulse energies and efficiencies of the three relevant driver designs for 4, 6 and 8 ns pulse widths. Comparing the two totem-pole drivers with the LR parallel driver with peaking, it becomes obvious that the latter reaches significantly better pulse energies and efficiencies at very short pulses of 4 ns. Especially the efficiency of the LM5134 totem-pole driver with high switching losses of approx. 5.1 mW at f_{pulse} = 100 kHz drops at very short pulses below 0.1%. However, at longer pulses of 8 ns, both totem-pole drivers begin to outperform the LR parallel driver in terms of pulse energy and efficiency.

5.4 | Peak Current Scalability

Pulse energy can be increased by higher peak currents if required. Within the presented experiments, LEDs were operated in LC and LR drivers, without observed damage, at 15–20 A, which is 5 to 6 times their peak current rating. Operation at more than 20 times the rated current has been reported previously [15]. However no evidence about long-term LED health can be derived, due to small sample size. While the LC and LR drivers with options for fast switching, high current GaN-FETs are practically limited by LED threshold, the totem pole drivers are limited by their supply voltage rating (12 V, LM5134) and internal resistance (1 Ω, LM5134). For the red LED, this limits the peak current to 7.6 A.

TABLE 2 | Driver efficiencies and pulse energies at different pulse widths, 3 A LED peak current and f_{pulse} = 100 kHz.

Driver	t_{fwhm} (ns)	Eff. (%)	E_{pulse} (nJ)
LR parallel with peaking	4	0.31	0.43
Totem-pole LM5134	4	0.06	0.05
Totem-pole LMG1020	4	0.46	0.11
LR parallel with peaking	6	0.38	0.76
Totem-pole LM5134	6	0.29	0.37
Totem-pole LMG1020	6	1.26	0.52
LR parallel with peaking	8	0.41	1.03
Totem-pole LM5134	8	0.62	1.16
Totem-pole LMG1020	8	1.96	1.27

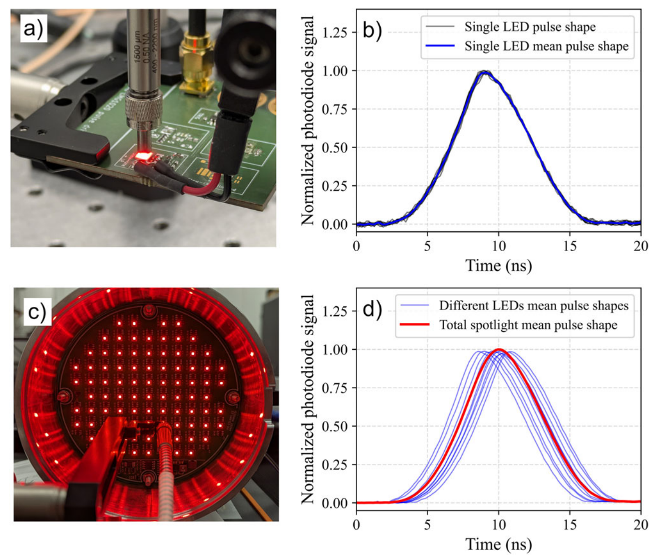

FIGURE 6 | (a) Single LED driver characterization setup, (b) single LED pulse variation, (c) spotlight with 89 LEDs in an 8x8 mm grid, and (d) pulse variation and mean pulse of 10 random LEDs within the spotlight.

6 | Large Array Spotlight

The single driver characterization showed that both inductive sweep-out and totem-pole drivers achieve 4–8 ns pulse widths. Even though, the LR driver outperforms the totem-pole driver in terms of fall time, an LM5134 totem-pole driver was selected for the realization of a spotlight with 89 LEDs (see demonstrator in Figure 6). For the intended application of the array spotlight (underwater lighting), it was critical to also support an efficient continuous wave CW operation and the LR-parallel driver efficiency falls far behind the totem-pole driver efficiency when approaching CW operation, because of the low impedance parallel path. Furthermore, the slightly faster rise and fall times of the LM5134 were preferred over the increased efficiency of the LMG1020. The 89 LED array achieves 62 mW average optical power at $t_{fwhm} = 6$ ns and $f_{pulse} = 1$ MHz. At 10 ns pulse width, the average power even increases to 294 mW.

In many applications like LiDAR, the stability of the pulse (including stability of the trigger pulse repetition rate $t_{prr} = 1/f_{pulse}$, optical pulse length t_{fwhm} and delay between trigger signal and emission t_d) is crucial. The trigger signal was measured to be stable within approx. half a nanosecond at a nominal pulse frequency of 1 MHz ($t_{prr} = 996.0$ ns $\pm$ 0.5 ns). The delay between trigger pulse and optical pulse (measured between both 50% rising edge levels) for a single LED varies by less than $\pm$125 ps (see measurement setup and results in Figures 6a and 6b). However, from one LED to another this delay variation increases up to $\pm$ 630 ps (see Figure 6d). This is predominantly caused by different copper path-lengths and component tolerances. The optical pulse width, on the other hand, hardly changes from LED to LED ($t_{fwhm} = 6.0 \pm 0.1$ ns). Consequently, the LED to LED fixed delay differences and the trigger jitter are the primary effects for broadening the optical pulse of the spotlight.

7 | Conclusion

The comparison of different nanosecond LED drivers for 3 A currents shows, that 4–8 ns optical pulses can be achieved with both inductive sweep-out measures and totem-pole drivers. The inductive sweep-out driver with current peaking excels with 2.5 ns fall time and highest pulse energy at very short 4 and 6 ns pulses, while the totem-pole drivers provides better efficiency and pulse energy at longer 8 ns pulses. Furthermore, the scalability is demonstrated with a totem-pole driver based spotlight consisting of 89 LEDs in an 8 $\times$ 8 mm grid. A pulse timing analysis showed the LED to LED fixed delay and trigger jitter becoming the primary effects broadening the optical pulse in a large array spotlight compared to a single LED. The ability to have high power LED spotlights capable of nanosecond pulses will enable new applications, for instance in underwater imaging and environmental sciences.

Author Contributions

Jendrik Schmidt: conceptualization, formal analysis, investigation, methodology, software, validation, visualization, writing – original draft. **Georg Ludwig:** formal analysis, investigation, methodology, validation, writing – review & editing. **Jan Menke:** conceptualization, investigation, writing – review & editing. **Enno Peters:** conceptualization, supervision, writing – review & editing. **Maurice Stephan:** resources, supervision, writing – review & editing. **Oliver Zielinski:** supervision, writing – review & editing.

Acknowledgements

Open access funding enabled and organized by Projekt DEAL.

Funding

The authors have nothing to report.

Conflicts of Interest

The authors declare no conflicts of interest.

Data Availability Statement

Data underlying the results presented in this paper are not publicly available at this time but may be obtained from the authors upon reasonable request.

References

1. C.-S. A. Gong, Y.-C. Lee, J.-L. Lai, C.-H. Yu, L. R. Huang, and C.-Y. Yang, "The High-Efficiency Led Driver for Visible Light Communication Applications," *Scientific Reports* 6, no. 1 (2016): 30991.

2. K. Modepalli and L. Parsa, "Active Pulse Shaping Circuit for Bandwidth Enhancement of High-Brightness LEDs Using GAN Devices," in *2018 IEEE Applied Power Electronics Conference and Exposition (APEC)* (IEEE, 2018), 3471–3476.

3. I. Gharib and M. Sawan, "High-Efficiency Led Driver for Short Fluorophores Lifetime Biosensing Applications," in *2019 17th IEEE International New Circuits and Systems Conference (NEWCAS)* (IEEE, 2019), 1–4.

4. T. Shiina, "Led Mini Lidar for Atmospheric Application," *Sensors* 19, no. 3 (2019): 569.

5. A. Maccarone, K. Drummond, A. McCarthy, et al., "Submerged Single-Photon Lidar Imaging Sensor Used for Real-Time 3D Scene Reconstruction in Scattering Underwater Environments," *Optics Express* 31, no. 10 (2023): 16690–16708.

6. A. Das and M. Pramanik, "Nanosecond Pulsed Current Source for Light Emitting Diode (LED) Driven Photoacoustic Signal Acquisition Systems," *Journal of Physics: Photonics* 7, no. 1 (2025): 015015.

7. T. J. Allen and P. C. Beard, "High Power Visible Light Emitting Diodes as Pulsed Excitation Sources for Biomedical Photoacoustics," *Biomedical Optics Express* 7, no. 4 (2016): 1260–1270.

8. T. Kishi, H. Tanaka, Y. Umeda, and O. Takyu, "A High-Speed LED Driver That Sweeps Out the Remaining Carriers for Visible Light Communications," *Journal of Lightwave Technology* 32, no. 2 (2014): 239–249.

9. H. Halbritter, C. Jager, R. Weber, M. Schwind, and F. Mollmer, "High-Speed LED Driver for NS-Pulse Switching of High-Current LEDs," *IEEE Photonics Technology Letters* 26, no. 18 (2014): 1871–1873.

10. P. Binh, T. Vo, C. T. Anh, et al., "Novel LED's Driver Circuit for Broadband Short-Range Optical Fiber Communication Systems," in *2012 4th International Conference on Communications and Electronics, ICCE 2012* (IEEE, 2012).

11. P. H. Binh, V. D. Trong, P. Renucci, and X. Marie, "Improving OOK Modulation Rate of Visible Led by Peaking and Carrier Sweep-Out Effects Using *n*-Schottky Diodes-Capacitance Circuit," *Journal of Lightwave Technology* 31, no. 15 (2013): 2578–2583.

12. O. Veledar, P. O. Byrne, S. Danaher, J. I. H. Allen, L. F. Thompson, and J. E. McMillan, "Simple Techniques for Generating Nanosecond Blue Light Pulses From Light Emitting Diodes," *Measurement Science and Technology* 18, no. 1 (2007): 131–137.

13. J. Schmidt, E. Peters, M. Stephan, and O. Zielinski, "Feasibility Study on LED-Based Underwater Gated-Viewing for Inspection Tasks," in *OCEANS 2022, Hampton Roads* (IEEE, 2022), 1–8.

14. J. Williams, "An98 - Signal Sources, Conditioners and Power Circuitry," 2004, https://www.analog.com/media/en/technical-documentation/application-notes/an98f.pdf.

15. C. Willert, B. Stasicki, J. Klinner, and S. Moessner, "Pulsed Operation of High-Power Light Emitting Diodes for Imaging Flow Velocimetry," *Measurement Science and Technology* 21, no. 7 (2010): 075402.